

Approaching the event horizon: 1.3mm λ VLBI of SgrA*

Sheperd Doeleman

MIT Haystack Observatory, Off Route 40, Westford, MA 01886, USA

E-mail: sdoeleman@haystack.mit.edu

Abstract. Advances in VLBI instrumentation now allow wideband recording that significantly increases the sensitivity of short wavelength VLBI observations. Observations of the super-massive black hole candidate at the center of the Milky Way, SgrA*, with short wavelength VLBI reduces the scattering effects of the intervening interstellar medium, allowing observations with angular resolution comparable to the apparent size of the event horizon of the putative black hole. Observations in April 2007 at a wavelength of 1.3mm on a three station VLBI array have now confirmed structure in SgrA* on scales of just a few Schwarzschild radii. When modeled as a circular Gaussian, the fitted diameter of SgrA* is $37\mu\text{as}$ ($+16, -10; 3\sigma$), which is smaller than the expected apparent size of the event horizon of the Galactic Center black hole. These observations demonstrate that mm/sub-mm VLBI is poised to open a new window onto the study of black hole physics via high angular resolution observations of the Galactic Center.

1. Introduction

At a distance of ~ 8 kpc ([1]), SgrA*, the compact radio, NIR and X-ray source at the Galactic Center, is thought to mark the position of a super-massive black hole of mass $\sim 4 \times 10^6 M_\odot$ ([2],[3]). Proper motions of SgrA* ([4]) confirm that it traces a significant amount of the mass that is inferred by stellar motions and orbits. Due to its proximity, SgrA* is the only galactic nucleus that can be studied with VLBI on sub-AU linear scales ($R_{\text{sch}} \sim 10\mu\text{as} \sim 0.1\text{AU}$). The ionized ISM, however, scatter-broadens images of SgrA* with a λ^2 dependence, and VLBI at the highest frequencies is the only available means to set important limits on intrinsic structures near the event horizon. VLBI at 7 mm and 3.5 mm has detected evidence for intrinsic structure of SgrA*, but these observations remain dominated by scattering effects, and the intrinsic sizes at these wavelengths (set by the optical depth of the emission) are much larger than the apparent size of the event horizon ([5], [6]). Evidence from light curves of SgrA* flares from the radio to Xray ([7], [8], [9]) implicate structures on smaller ($\sim 5 - 15R_{\text{sch}}$) scales. Only at frequencies above 230GHz does the scattering size become smaller than the VLBI array resolution allowing direct measurement of intrinsic structure on these scales corresponding to the innermost accretion region. Over the past decade, MIT Haystack Observatory has focused on developing next-generation wideband VLBI instrumentation capable of significantly increasing the sensitivity of mm/submm VLBI arrays. The observations described herein used this instrumentation to show that 1.3mm VLBI of SgrA* can now probe the event horizon of this super-massive black hole candidate.

2. Instrumentation

The focus of new VLBI instrumentation has been to process higher bandwidths using commercially available digital technology. For VLBI, this has translated into a re-conceptualization of the two main components of the traditional VLBI backend: the digitization/formatting stage and the recording stage.

2.1. Digital Backend

Prior to recording data for subsequent correlation, the IF (intermediate frequency) at each VLBI telescope must be sampled and channelized in frequency. The Mark4 system (similar to the system in use at the VLBA) uses a bank of analog filters to break the IF into sub-bands. With the advent of mature FPGA (Field Programmable Gate Array) technology, it is now feasible to channelize the IF signal using a polyphase filterbank approach that is realized in digital signal processing after the sampling stage. A collaboration between Haystack Observatory and the Space Science Laboratory at UC Berkeley has focused on developing a fully digital FPGA-based VLBI backend, which produces an output suitable for recording on modern hard-disk based recorders. This system, the DBE, is capable of sampling two 480MHz wide IFs, and producing two 2Gigabit/sec output streams (Nyquist sampled, 2-bit resolution). The DBE (Figure 1) represents a reduction in backend cost by a factor of ~ 10 over the previous Mark4 data acquisition system and is 5 times smaller in size (the size of a single PC). The next-generation DBE (imaginatively called DBE2), is currently under development, and will use the Xilinx Virtex5 family of FPGA chips to double the data throughput to ~ 8 Gigabits/sec.



Figure 1. The Digital Backend (DBE) system developed to process two 480MHz wide IF bands, producing an aggregate VLBI data output rate of 3.84 Gigabit/sec.

2.2. Mark5 Recorder

The Mark5 system was developed at Haystack Observatory in collaboration with Conduant Corp as the first high-data-rate VLBI data system based on magnetic-disc technology. Incorporating primarily low-cost PC-based components, the Mark5 system now supports data rates up to 2048 Mbps, recording to an array of 8 inexpensive removable hard disks. The Mark 5 system (Figure 2) was developed primarily to re-packaged the disks into convenient '8-pack' modules and over 100 Mark5 units are in use throughout the VLBI community. Support for Mark 5 development at MIT Haystack Observatory was provided by BKG, EVN, KVN, MPI, NASA, NRAO, NSF,

and USNO. The Mark5 system replaces a magnetic tape system, which used a non-standard reel-to-reel recorder and a special-purpose tape media whose cost was not likely to decrease over time. The new system is over a factor of 5 smaller in size than the previous recorder with a data rate improvement of x4. The cost for this new recording system is ~ 10 times less than the tape system and uses standard commercial disk media whose cost (per GigaByte) is projected to substantially decrease over time. Efforts to increase recording rates to 4Gigabits/sec are underway, and the new Mark5C recorder will be capable of recording data from 10Gigabit Ethernet inputs.

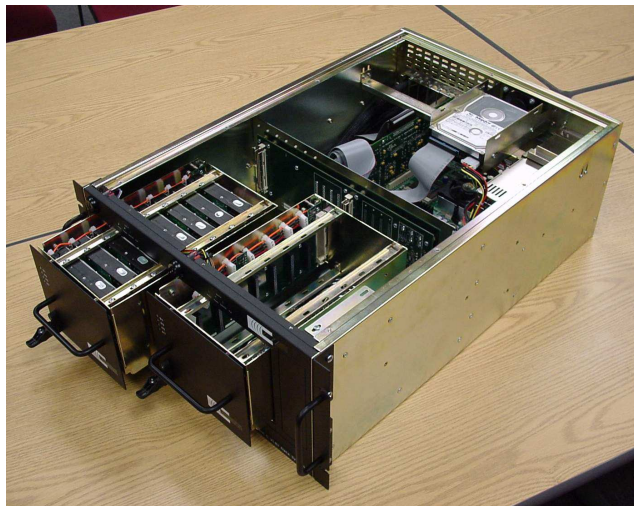


Figure 2. The Mark5 hard disk VLBI data recorder. Each hard disk module holds up to 8 individual hard disks. With current disk sizes, a full module can record 6 TBytes. Maximum recording rates are now 2Gb/s but will increase to 4Gb/s in 2009.

3. Observations

In April 2007, SgrA* and several quasar calibrators were observed over two consecutive days at a wavelength of 1.3mm with a three station VLBI array ([10]). The array included the James Clerk Maxwell Telescope (JCMT) on Mauna Kea, the Arizona Radio Observatory Submillimeter Telescope (ARO/SMT) on Mt Graham in Arizona, and one 10m dish of the Coordinated Array for Research in Millimeter-wave Astronomy (CARMA) in California. Projected baseline lengths on SgrA* ranged from $500 \times 10^6 \lambda$ on the shortest baseline to $3500 \times 10^6 \lambda$ on the longest. An effective bandwidth of 960 MHz was recorded, resulting in an aggregate recording data rate of 3.84 Gigabits/sec at each site (2 bits/sample, Nyquist sampling). Data were processed on the MIT Haystack Observatory Mark4 Correlator to produce complex visibilities with 0.5 second time resolution. Calibration quasars were robustly detected on all three baselines, validating operation of the VLBI array and allowing refinement of telescope positions for processing of the SgrA* observations.

Because the geometry of VLBI baselines in an array is not typically known to $\ll 1\lambda$ precision, it is standard practise to search for detections over a grid of interferometric delay and delay-rate. A peak in signal-to-noise ratio of the visibility amplitude, found over a range of Nyquist-sampled delay and delay-rate space, is deemed a detection if the probability of false detection is sufficiently low. At an observing wavelength of 1.3mm, atmospheric turbulence limits the time over which the VLBI signal can be coherently integrated. Therefore, a technique of incoherent averaging ([11]) was used, to perform the fringe search over each 10 minute VLBI scan and to

determine the VLBI signal amplitude. Incoherent averaging extends the effective integration time, but builds signal to noise more slowly than \sqrt{t} . After measuring the coherence losses due to atmospheric effects over a range of time scales, the atmospheric coherence time was found to be ~ 8 seconds, and the VLBI detection searches were thus made by incoherently averaging 8 second intervals of coherently averaged data. These searches resulted in robust detections and correlated flux density measurements of SgrA* on both the ARO/SMT-JCMT and ARO/SMT-CARMA baselines (see Figure 3). No detections were found on the CARMA-JCMT baseline, which is attributable to the lower sensitivity of that baseline compared with the others. The error associated with each visibility amplitude was calculated by adding in quadrature the noise determined from the detection search with a 10% calibration error. Measurements of SgrA* made with the CARMA array during the VLBI observations yield a total flux density of SgrA* of 2.4 ± 0.25 Jy, which was observed to be stable over both days, suggesting that SgrA* was observed in a quiescent state. Errors in the total flux density measurement are dominated by pointing and calibration.

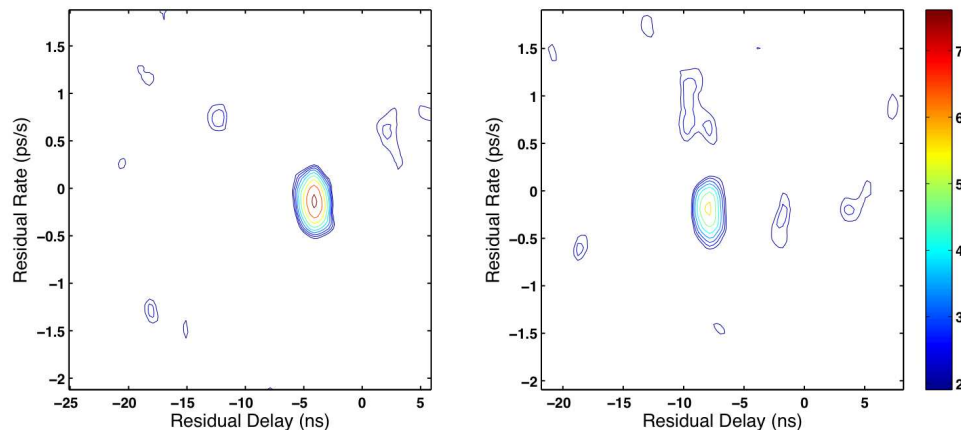


Figure 3. Detections of SgrA* and nearby calibrator at $1.3\text{mm}\lambda$ on a 3500km projected baseline between the Submillimeter Telescope on Mt. Graham, AZ and the James Clerk Maxwell Telescope on Mauna Kea, HI. Shown are searches in signal to noise ratio over interferometer delay and delay-rate for 10 minute scans for quasar PKS B1921-293 on April 11, 2007 at 14:00UT (left) and for SgrA* the same day at 12:00UT (right). The data were segmented into 8 second intervals to reduce coherence loss due to atmospheric turbulence and the amplitudes were averaged incoherently. The formal probability of false detection (PFD) in each search is computed by comparing the observed signal to noise ratio with maximal peaks derived from pure noise over the same search space, and is $< 10^{-9}$ for both fringe searches shown above. Contours in each plot begin at signal to noise ratio of 2.0 and increase in steps of $2^{1/4}$. Peak signal to noise is 7.9 and 5.8 on the left and right searches respectively.

4. Discussion

A circular Gaussian model was fit to the VLBI data (shown in Figure 4). The weighted least-squares best-fit model has a total flux density of 2.4 ± 0.5 Jy and full width at half maximum (FWHM) of $43 (+14,-8) \mu\text{as}$ where errors are 3σ . On the assumption of a Gaussian profile, the intrinsic size of Sgr A* can be extracted from our measurement assuming that the scatter broadening due to the ISM adds in quadrature with the intrinsic size. At a wavelength of 1.3 mm the scattering size extrapolated from previous longer-wavelength VLBI ([12]) is $\sim 22\mu\text{as}$.

Removing the scattering effects results in a 3σ range for the intrinsic size of Sgr A* equal to $37 (+16, -10) \mu\text{as}$. The 3σ intrinsic size upper limit at 1.3 mm, combined with a lower limit to the mass of Sgr A* of $4 \times 10^5 M_\odot$ from measured proper motions yields a lower limit for the mass density of $9.3 \times 10^{22} M_\odot \text{pc}^{-3}$. This density lower limit and central mass would rule out most alternatives to a black hole for Sgr A* because other concentrations of matter would have collapsed or evaporated on timescales that are short compared with the age of the Milky Way ([13]).

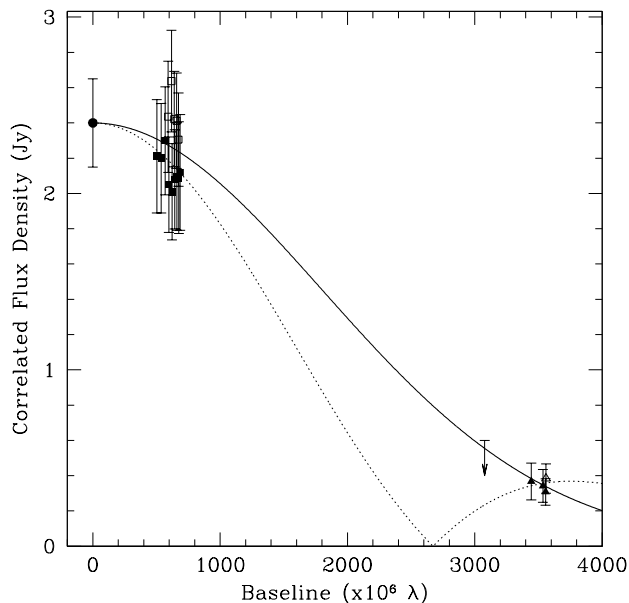


Figure 4. Shown are the correlated flux density data on the ARO/SMT-CARMA and ARO/SMT-JCMT baselines plotted against projected baseline length (errors are 1σ). Squares show ARO/SMT-CARMA baseline data and triangles show ARO/SMT-JCMT data, with open symbols for 10 April and filled symbols for 11 April. The solid line shows the weighted least-squares best fit to a circular Gaussian brightness distribution, with FWHM size of $43.0 \mu\text{as}$. The dotted line shows a uniform thick-ring model with an inner diameter of $35 \mu\text{as}$ and an outer diameter of $80 \mu\text{as}$ convolved with scattering effects due to the interstellar medium. The total flux density measurement made with the CARMA array over both days of observing is shown as a filled circle. An upper limit for flux density of 0.6 Jy , derived from non-detection on the JCMT-CARMA baselines, is represented with an arrow near a baseline length of $3075 \times 10^6 \lambda$.

It should be noted, however, that while structure on $4R_{\text{Sch}}$ scales is present in SgrA*, models other than the circular Gaussian can be fit to the data. This is illustrated by the dotted line in Figure 4, which shows the expected flux density as a function of baseline length for a uniform circular annulus with inner diameter $35 \mu\text{as}$ and outer diameter $80 \mu\text{as}$ that has been scatter broadened by the ISM. Future higher-sensitivity observations will distinguish between these two models by allowing detections of SgrA* on the CARMA-JCMT baseline, which is now represented in Figure 4 only as an upper limit.

Because of gravitational lensing effects due to the extreme gravity near the assumed black hole, radiation emitted from near the event horizon of a non-spinning black hole will have an apparent size of $3\sqrt{3}R_{\text{Sch}}$. For SgrA*, this expected diameter is $5.2R_{\text{Sch}} \simeq 52 \mu\text{as}$, which differs by 3σ from the size derived from a Gaussian model. Even if the black hole is maximally spinning

($a=1$), the diameter of the event horizon in the equatorial plane ($\sim 45\mu\text{as}$) would still exceed the estimated size. This suggests that SgrA* is not an optically thick emission region that symmetrically enfolds the black hole. Rather, it is likely due either to emission from a jet or from the approaching (and therefore Doppler enhanced) side of an accretion disk that is inclined to our line of sight ([14], [15], [16]). Either scenario results in emission that is offset from the black hole position. This marks the first time that astronomical observations of any kind have directly constrained the spatial relationship between SgrA* and the black hole.

5. Conclusions

The technology to significantly increase the sensitivity of VLBI at wavelengths of 1.3mm and shorter is now enabling observations of SgrA* on Schwarzschild radius scales. Efforts to extend the capabilities of the current 1.3mm VLBI array include: phasing together radio telescopes on Mauna Kea and at CARMA to increase collecting area (discussed elsewhere in these proceedings), continuing to pursue increases in recording bandwidth, and bringing new mm/submm VLBI sites on-line.

By 2009, the international collaboration (see the author list of [10]) that has carried out these observations, will field a higher sensitivity 1.3mm VLBI array that will be sensitive to time variable structures in SgrA*. The closure phase is the sum of interferometric phases around a triangle of baselines, is largely immune from calibration errors, and deviates from zero in the presence of asymmetric source structure. Projected sensitivities will allow monitoring of the closure phase on ~ 10 second time scales, and enable tests for periodic structure variation in SgrA* as is predicted by orbiting hot-spot models of the accretion flow ([16], [17]). By timing periodicities in the closure phase, one can extract the fundamental black hole spin parameter ([18]). Thus, by spatially resolving the innermost accretion region surrounding SgrA*, mm/submm VLBI is now positioned to address fundamental issues in black hole physics.

Acknowledgments

VLBI at mm/submm wavelengths would not be possible without the dedicated support of staff and scientists at all participating facilities. VLBI work at the MIT Haystack Observatory is supported through grants from the National Science Foundation.

References

- [1] Reid M 1993 *ARA&A* **31** 345
- [2] Schödel R et al 2002 *Nature* **419** 694
- [3] Ghez A M et al 2005 *ApJ* **620** 744
- [4] Reid M J & Brunthaler A 2004 *ApJ* **616** 872
- [5] Bower G C, Falcke H, Herrnstein R M, Zhao J H, Goss W M & Backer D C 2004 *Science* **304** 704
- [6] Shen Z Q, Lo K Y, Liang M -C, Ho P T P & Zhao J-H 2005 *Nature* **438** 62
- [7] Eckart A et al 2006 *A&A* **450** 535
- [8] Yusef-Zadeh F et al 2006 *ApJ* **644** 198
- [9] Marrone D et al 2008 *ApJ* **682** 373
- [10] Doeleman S. S et al 2008 *Nature* **455** 78
- [11] Rogers A E E, Doeleman S & Moran J M 1995 *AJ* **109** 1391
- [12] Bower G C et al 2006, *ApJ* **648** L127
- [13] Maoz E 1998 *ApJ* **494** L181
- [14] Falcke H, Melia F & Algol E 2000 *ApJ* **528** L13
- [15] Noble S C, Leung, P K, Gammie, C F & Book, L G 2007 *Class. Quant. Gravity* **24** S259
- [16] Broderick A E & Loeb A 2006b *MNRAS* **367** 905
- [17] Genzel R et al 2003 *Nature* **425** 934
- [18] Doeleman S S, Fish V L, Broderick A E, Loeb A & Rogers A E E 2008 *Preprint astro-ph/0809.3424*